9th AUSTRALASIAN
FLUID MECHANICS CONFERENCE,
AUCKLAND, 8-12 DECEMBER 1986

Lagrangian Statistical Simulation of Turbulent Dispersion in the Convective Boundary Layer

B. L. SAWFORD and F. M. GUEST

CSIRO Division of Atmospheric Research

ABSTRACT

A generalized Langevin model is used to conduct Lagrangian statistical simulations of turbulent dispersion in a shear-free convective boundary layer.

For instantaneous area sources mean concentration predictions compare very favourably with convection tank data. Diffusivities calculated for a near-surface source also agree very well with convection tank data and show substantial regions of counter-gradient flux. Calculations for other source heights also show regions of counter-gradient flux and confirm that the diffusivity is a strong function of source height.

For continuous area sources model predictions are in excellent agreement with the results of large-eddy simulations. They show that there is a strong asymmetry between 'top-down' and 'bottom-up' dispersion processes and that the bottom-up process has a substantial region of counter- gradient flux in the upper half of the boundary layer.

INTRODUCTION

Turbulent transfer in the atmospheric convective boundary layer (CBL) is complicated by a number of features of the vertical structure of the turbulence. These include asymmetry between up-drafts and down-drafts (causing the vertical velocity distribution to be significantly skewed), the size of the eddies (comparable with the depth of convection) and the strong inhomogeneity, particularly near the ground. As a result turbulent dispersion is non-local and non-Gaussian and cannot be described by simple Gaussian-plume and K-theory models.

Recently, statistical models of dispersion have been developed to incorporate these properties of the turbulence. The analytical statistical models of Misra (1982) and Venkatram (1983) and the numerical model of Weil and Furth (1982) treat the vertical component of turbulence as homogeneous and positively skewed and assume that, except for reflection at the top and bottom boundaries, fluid elements (marked particles) always move with their initial velocity (drawn from the velocity distribution of the turbulence at the source height). Although these models ignore the effect of a finite Lagrangian velocity time scale and inhomogeneity of the turbulence near the surface and the top of the boundary layer, they capture much of the essential physics of dispersion from elevated sources in the CBL.

Full Lagrangian simulations (based on the Langevin equation as a model for particle velocities) which incorporate a finite Lagrangian time scale and inhomogeneity of the turbulence have recently been carried out by Baerentsen and Berkowicz (1984) and de Baas et al. (1986). Their simulations are in excellent agreement with the laboratory convection tank data for the mean concentration field.

In the present paper we use a modified form of the de Baas et al. model and focus on flux-gradient relationships (and their breakdown) in the CBL. In particular we examine the performance of our model in describing the non-local features of turbulent dispersion in the CBL for both instantaneous and continuous area source distributions.

MODEL FORMULATION

The Lagrangian stochastic approach to turbulent dispersion is now fairly well-known and so will only be described briefly (see Sawford (1985) for a recent overview). Basically, statistics of the concentration field are calculated as moments of the joint probability distribution for the position and velocity of marked fluid particles. In particular, for an arbitrary source distribution, $C_s(z_o,t_o)$, the moments $\overline{w^n C}$ are

$$\overline{w^n C}\,(z,t) = \int_o^t \iiint w^n P(w,z,t;\, z_o,t_o) C_s(z_o,t_o)\, dz_o\, dt_o\, dw \qquad (n=0,1,2\ldots) \qquad (1)$$

where $C = \bar{C} + c$ and $P(w,z,t;\, z_o,t_o)$ is the probability density that a particle initially at z_o with a velocity drawn from the turbulence velocity distribution at z_o is observed between z and z + dz with velocity between w and w + dw at time t. With n=0 (1) reduces to the well-known result for the mean concentration, $\bar{C}$. In practice the moments are calculated as averages (of w^n) over independent particle trajectories distributed according to P and C_s. The problem is, of course, to ensure that the modelled trajectories are appropriately distributed.

Here we model particle trajectories with a generalization of the Langevin equation which involves non-Gaussian random forcing. In particular we write

$$\left.\begin{aligned} d\tilde{W} &= \frac{-\tilde{W}}{T_L(Z,t)}\, dt + d\omega_{Z,t} \\ \text{and} \quad dZ &= W\, dt = \sigma_w(Z,t)\, \tilde{W}\, dt \\ \text{with} \quad \langle (d\omega_{Z,t})^n \rangle &= \frac{a_n(Z,t)}{\sigma_w^n(Z,t)}\, dt \quad (n=1,2,\ldots) \\ \text{and} \quad \sigma_w^2 &= W^2 \quad . \end{aligned}\right\} \qquad (2)$$

Z and W are the vertical components of the position and velocity respectively of a marked fluid element, T_L is a time scale over which W is correlated and $d\omega_{Z,t}$ is a general random forcing. The notation $\langle\ \rangle$ represents an ensemble average for fixed Z,t subject to the initial conditions Z(o)=z_o and that W(o) be chosen from the distribution at z_o of the Eulerian velocity component, w. Eulerian averages, denoted by $\overline{(\ )}$, correspond to initial conditions which represent an unbiased sample of fluid element positions and velocities at the initial time. In general we denote variables

representing a trajectory in (w,z) space by upper-case symbols and the independent variables by lower case symbols. Our trajectory model (2) is a rescaled version of the generalized Langevin equation used by de Baas et al. (1985).

The random forcing moments (i.e. the a_n) can be expressed in terms of Eulerian moments of the turbulence by requiring that the model satisfy the 2nd Law of Thermodynamics i.e. that an initially well-mixed state should remain so (Sawford, 1986). A corollary of this constraint is that in bounded turbulence the steady-state concentration distribution should be homogeneous. For a general, non-stationary, inhomogeneous non-Gaussian turbulence the a_n satisfying the 2nd Law are given by (Sawford, 1986)

$$a_n = \frac{\partial \overline{w^n}}{\partial t} + \frac{\overline{nw^n}}{T_L} + \sigma_w^n \frac{\partial}{\partial z}\left(\frac{\overline{w^{n+1}}}{\sigma_w^n}\right) - \frac{\overline{w^n}}{\sigma_w^n}\frac{\partial \sigma_w^n}{\partial t} - \sum_{\nu=1}^{n-1}\binom{n}{\nu} a_\nu \overline{w^{n-\nu}} \qquad (n=1,2\ldots) \qquad (3)$$

Thus, given the Eulerian moments of the turbulence (and a parameterization for T_L) we can in principle determine the a_n which satisfy the 2nd Law of Thermodynamics.

For non-Gaussian turbulence, the forcing (3) is non-Gaussian. It is impractical to correctly specify all the a_n and in any case we rarely know more than the first three moments of the turbulence. Consequently, in practice the random forcing required by the 2nd Law of Thermodynamics can only be approximated and we expect departures from the uniform steady state concentration distribution. However, numerical tests show that the steady state distribution is within 5% of well-mixed for our model and that spurious concentration gradients are negligible.

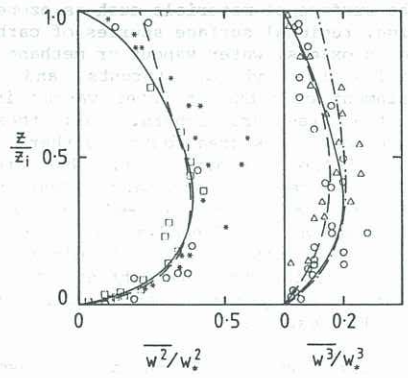

Fig.1: Turbulence parameterizations for the CBL. Eq.(4), (——); Baerentsen and Berkowicz (and de Baas et al. $\overline{w^2}$), (---); de Baas et al. $\overline{w^3}$, (-·-). Data points as in Baerentsen and Berkowicz.

We parameterize the variance and skewness of the turbulent vertical velocity in the CBL by

$$\left.\begin{aligned} \overline{w^2}/w_*^2 &= 1.1\,(z/z_i)^{2/3}(1-z/z_i)^{2/3}\left(1-\frac{4(z/z_i-0.3)}{(2+|z/z_i-0.3|)^2}\right) \\ \text{and}\quad \overline{w^3} &= 0.8\,\sigma_w^3 \end{aligned}\right\} \qquad (4)$$

where w_* is the convective velocity scale and z_i the depth of convection. These are plotted in Figure (1) together with the parameterizations used by Baerentsen and Berkowicz (1984) and by de Baas et al. (1985) and with laboratory and field data. Clearly the scatter in the data is sufficient to encompass a range of such parameterizations.

The time scale T_L is parameterized by

$$T_L\, w_*/z_i = \alpha\, \sigma_w^2/w_*^2 \qquad (5)$$

which satisfies free-convection similarity for $z \ll z_i$. It is also equivalent to a constant rate of dissipation of turbulence kinetic energy throughout the CBL as is observed to a good approximation. We have chosen $\alpha = 2.5$ but the results are not very sensitive to $2 < \alpha < 3$. The equations of motion are discretized using the simple Euler differencing scheme for which (2) becomes

$$\tilde{W}_{n+1} = \tilde{W}_n\left(1-\Delta t/T_L(Z_{n+1})\right) + \Delta\omega_{Z_{n+1}}$$

and $$Z_{n+1} = Z_n + \sigma_w(Z_n)\,\tilde{W}_n\,\Delta t\ , \qquad (6)$$

with $\Delta t = 0.02\,T_L$. $\Delta\omega$ is a random number with moments $a_n\Delta t$ given by (3). All the statistics reported in this paper are averages over 10^5 particle trajectories.

Skewed distributions are modelled as in de Baas et al. as the weighted sum of two Gaussians with mean and standard deviations $m_1 = \sigma_1$ and $m_2 = -\sigma_2$ respectively.

INSTANTANEOUS AREA SOURCES

We consider the vertical dispersion as a function of time, of a horizontally homogeneous instantaneous source located at height z_s. Although this is a rather idealized source distribution our results are directly comparable with the cross-wind integrated convection tank data of Willis and Deardorff (1976). Subject to the constraints of horizontal homogeneity and negligible wind shear they are also relevant to the more practical problems of dispersion from a continuous crosswind line source or to the crosswind-integrated dispersion from a continuous point source, so long as the streamwise intensity of turbulence is low. Our results are presented as functions of the non-dimensional time $X = tw_*/z_i$ which in the Taylor approximation is equivalent to $X = (x/U)\,w_*/z_i$, where U is the mean wind speed.

It follows from (1) that for an instantaneous area source $\overline{w^n C} = \overline{w^n c} + \overline{w^n}\,\bar{C}$ is just the average of w^n over all particles released from z_s at time t_s which arrive at z at time t. Recall that n = 0 gives the mean concentration, $\bar{C}$.

Figures 2(a) and (b) show mean concentration and flux contours for a source at $0.067\,z_i$. The $\bar{C}$ contours show that beyond $X \sim 0.5$ the locus of maximum concentration rises away from the surface. This 'lift-off' phenomenon, is a clear manifestation of the non-diffusive nature of transport in the CBL. Sawford (1984) found similar behaviour in a strongly inhomogeneous analogue of a neutral boundary layer and concluded that it is a consequence of a large vertical gradient in the length scale of the turbulence (i.e. in $\sigma_w T_L$). It is clear from (4) and (5) that near the ground this quantity indeed varies rapidly with height. The mean concentration field is practically well-mixed by $X \sim 3$.

As might be expected, the flux contours are much clearer indicators of turbulent transport than the corresponding concentration contours. In particular, the updraft and downdraft contributions stand out much more clearly as do reflections at the boundaries. The flux is negligible beyond $X \sim 3$.

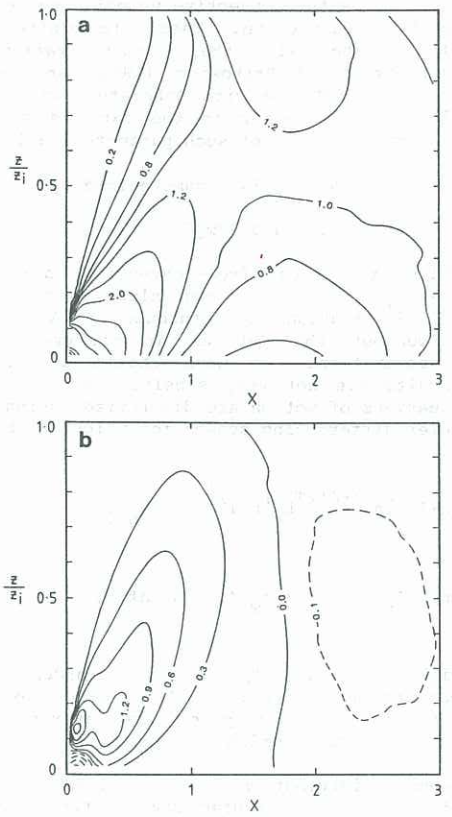

Fig.2: Concentration (a) and flux (b) contours for an instantaneous area source at $z_s = 0.067\ z_i$.

Inspection of the model results in Figure 2 shows that the loci of maximum concentration (where $\partial\bar{C}/\partial z=0$) do not coincide with the zero-flux lines. Consequently there are regions of counter-gradient flux and negative diffusivity. These are associated with the interaction of 'direct' and 'reflected' lobes of the updraft and downdraft plumes (this is most easily seen from the flux contours). Essentially, particles arriving at a given point can have widely differing transport histories (depending on whether they arrive directly or through a reflection) and hence can have widely differing effective diffusivities. In the present case these differences are due to the inhomogeneity of the turbulence, but counter-gradient fluxes are possible even in homogeneous turbulence when particles arriving at a given location have different effective diffusivities because of different release times and locations (Raupach, 1985).

Diffusivity contours calculated for $z_s = 0.067\ z_i$ are shown in Figure 3(a). In Figure 3(b) we have plotted contours of the diffusivity calculated by Deardorff and Willis (1975) from their water tank data. The correspondence between our calculations and the water tank data is remarkably good with the main region of negative diffusivity aligned along the lower side of the reflected down-draft concentration lobe. At the left hand boundary of this region the diffusivity diverges through $\pm\infty$ since the gradient vanishes there. At the right-hand boundary it changes sign through zero as the flux changes sign. There is also a small region of negative diffusivity associated with the upper side of the reflection of the updraft lobe from the top boundary where the flux and gradient are both negative. The model results also show a region of negative diffusivity near the top for $0.5 < X < 1.5$ which is not present in the laboratory data. This is probably an artifact of the rigid boundary assumed in the model; in the laboratory experiments entrainment of fresh fluid through the interface ensures a positive concentration gradient there.

The concentration fields calculated for sources at $0.24\ z_i$ and $0.49\ z_i$ also agree very well with convection tank data. These calculations show the diffusivity to be a strong function of source height.

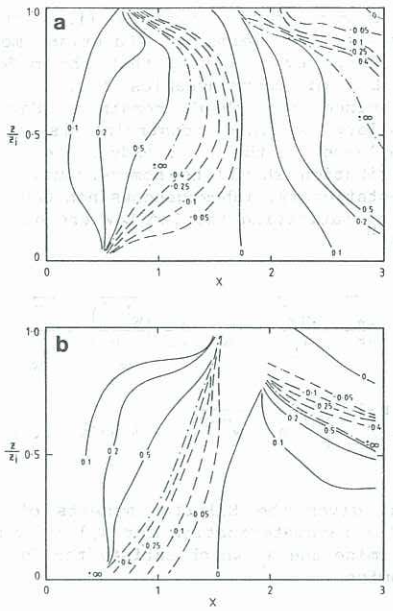

Fig.3: Model (a) and laboratory (b) diffusivity contours for the source in Fig.2.

CONTINUOUS AREA SOURCES

Here we consider the dispersion of scalar material released into (or extracted from) the convectively mixed boundary layer by continuous area sources (or sinks). Typical examples of practical interest are regional dry deposition processes involving a flux to the surface of materials such as ozone or sulphur dioxide, regional surface sources of carbon dioxide, nitrogen oxides, water vapour or methane from crops, agricultural land or forests and interfacial entrainment of ozone or water vapour into the CBL from the free troposphere. All these examples involve continuous area sources either at the top or bottom of the boundary layer. Wyngaard and Brost (1984) and Moeng and Wyngaard (1984) have studied these processes using large-eddy simulations (LES) and have shown that depending on the source configuration the 'mixed-layer' may be distinctly unmixed. Here we examine the predictions of our Langevin model for these processes and compare them with the large-eddy results.

For an area source with constant release rate (i.e. a constant source flux) (1) reduces (for unit source flux) to

$$\overline{w^n C}\ (z,t) = \int_0^t \overline{w^n C}\ (z,t,t_s)\ dt_s \qquad (7)$$

where $\overline{w^n C}\ (z,t,t_s)$ is the flux at height z and time t due to an instantaneous source released at time t_s. That is, the continuous area source fluxes can be obtained merely by integrating the instantaneous source result (or in discrete form by summing fluxes from a series of instantaneous sources). Recall that n = 0 returns the mean concentration $\bar{C}\ (z,t)$. In the previous Section we observed that the instantaneous source flux and mean concentration essentially converge to their asymptotic values after a non- dimensional time $X-X_s \sim 3$. Thus the corresponding continuous source quantities also reach steady state by $X \sim 3$. The results we present here are for X = 4, and integration to larger time shows no significant changes.

As noted by Wyngaard and Brost (1984) the flux profile is constrained by the relation

$$\frac{\partial \bar{C}}{\partial t} = \frac{-\partial}{\partial z} \overline{wc} \qquad (8)$$

to be linear in z once the concentration gradient reaches steady state. Since our model satisfies (8) exactly (Sawford (1986)), a linear flux profile is assured regardless of the detailed properties of the turbulence. Thus, the flux profile reflects little of the interesting and complex features of the turbulence and the transport processes. These are manifested instead through the mean concentration distribution.

Normalized concentration gradients, $g=-(\partial \bar{C}/\partial z)z_i/c_*$, for top-down and bottom-up dispersion calculated from our model are shown in Figure 4(a) together with the LES results of Moeng and Wyngaard (1984). Considering the differences in the calculation procedures and the uncertainties involved in our turbulence parameterizations, and in sub-grid scale processes in the LES, the correspondence between these two sets of results is remarkable. Our bottom-up gradient is generally weaker and changes sign (corresponding to a counter-gradient flux) a little lower in the boundary layer, but otherwise shows all the features of the large-eddy result. That we have been able to reproduce this counter-gradient flux and the increasing concentration gradient at the top of the CBL is particularly reassuring since the differences between the large-eddy results of Wyngaard and Brost and Moeng and Wyngaard suggests that these are quite sensitive features to model.

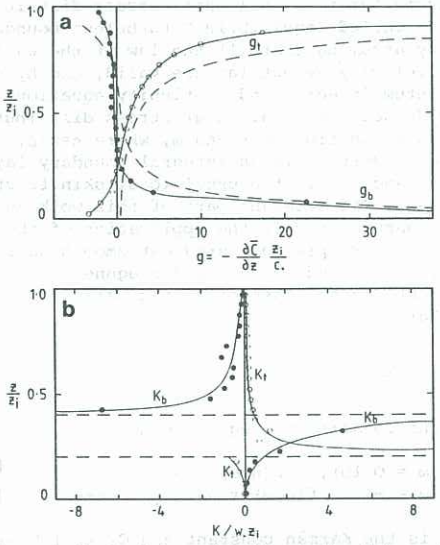

Fig.4: Gradient (a) and diffusivity (b) profiles for continuous area sources at the top (t) and bottom (b) of the CBL. In (a) the broken lines show the LES results of Moeng and Wyngaard.

Our results show the top-down gradient to be generally larger than the bottom-up gradient, in agreement with the LES data, but also show a small region of negative gradient near the bottom boundary which is not present in the LES results. Tests with different turbulence parameterizations suggest that this may be due to an underestimation of w^3 by (4).

As noted by Wyngaard and Brost (1984) and Moeng and Wyngaard (1984) the top-down and bottom-up processes are far from symmetrical. In fact the results show two sorts of asymmetry. Firstly the gradient profiles are not symmetrical about $z/z_i = 0.5$ This is due simply to an asymmetric diffusivity profile and would result even from a first order closure model with a prescribed asymmetric diffusivity. Secondly the top-down and bottom-up diffusivity profiles are different. This is emphasized in Figure 4(b) which shows diffusivity profiles calculated from our model results. The dependence of the diffusivity on the source-height in this way is a consequence of the non-diffusive nature of the turbulent transfer, as are the regions of negative diffusivity.

CONCLUSIONS

We have applied a generalized Langevin model to the calculation of dispersion in the shear-free convective boundary layer.

Mean concentration predictions for instantaneous area sources at various heights in the convective boundary layer are in excellent quantitative agreement with laboratory convection tank data. We have also made calculations of the concentration flux for these instantaneous sources and so determined the effective turbulent diffusivity. For a near surface source the calculated diffusivity field is in excellent agreement with that inferred by Deardorff and Willis (1975) from convection tank data. Our calculations also show the diffusivity to be a strong function of source height.

By integrating the instantaneous source results over time we have also calculated concentration statistics for continuous area sources. The main point of interest is the difference between dispersion from the top and bottom of the CBL. Our results are in excellent agreement with the LES results of Moeng and Wyngaard (1984) and show a strong asymmetry between top-down and bottom-up dispersion. In particular, the bottom-up process has a region of counter-gradient flux in the upper portion of the boundary layer where the gradient and flux are both positive.

REFERENCES

de Baas, A.F., H. van Dop and F.T.M. Nieuwstadt, 1985: An application of the Langevin equation for inhomogeneous conditions to dispersion in a convective boundary layer. Quart.J.Roy.Meteor. Soc., 112, 165-180.

Baerentsen, J.H. and R. Berkowicz, 1984: Monte Carlo simulation of plume dispersion in the convective boundary layer. Atmos.Environ., 18, 701-712.

Deardorff, J.W. and G.E. Willis, 1975: A parameterization of diffusion into the mixed layer. J.Appl.Meteor., 14, 1451-1457.

Misra, P.K., 1982: Dispersion of non-buoyant particles inside a convective boundary layer. Atmos.Environ., 16, 239-243.

Moeng, C.-H. and J.C. Wyngaard, 1984. Statistics of conservative scalars in the convective boundary layer. J.Atmos.Sci., 41, 3162-3169.

Raupach, M.R., 1985: Transport of scalar constituents in vegetation canopies: A Lagrangian analysis. Proc. Third Australian Conference on Heat and Mass Transfer, University of Melbourne

Sawford, B.L., 1984: Lagrangian statistical modelling of turbulent dispersion, Proc.Eighth Int.Clean Air Conf., Melbourne, Clean Air Society of Australia and New Zealand, 17-27.

Sawford, B.L., 1985: Lagrangian statistical simulation of concentration mean and fluctation fields. J.Clim.Appl.Meteor, 24, 1152-1166.

Sawford, B.L., 1986: Generalized random forcing in random walk turbulent dispersion models, Phys. Fluids (in press).

Venkatram, A., 1983: On dispersion in the convective boundary layer. Atmos.Environ. 17, 529-533.

Weil, J.C. and W.F. Furth, 1981: A simplified numerical model of dispersion from elevated sources in the convective boundary layer. Proc Fifth Symp. on Turbulence, Diffusion and Air Pollution, Atlanta, Amer.Meteor.Soc., 76-77.

Willis, G.E. and J.W. Deardorff, 1976: A laboratory model of diffusion into the convective planetary boundary layer. Quart.J.Roy.Meteor.Soc., 102, 427-445.

Wyngaard, J.C. and R.A. Brost, 1984: Top-down and bottom-up diffusion of a scalar in the convective boundary layer, J.Atmos.Sci. 41, 102-112.